

Spanwise Velocity Distributions in Jets from Rectangular Slots

G. F. Marsters*

Queen's University at Kingston, Kingston, Ontario, Canada

Turbulent jet flows from rectangular nozzles exhibit "saddle-backed" velocity profiles that are related to the upstream shaping of the nozzles. These velocity peaks are as much as 20% greater than the centerline velocity. The peaks appear to merge downstream. The present study includes examination of the mean and turbulence velocities of the jets for which strong peaks are evident. Contour plots of the mean velocity fields are presented. Outputs from two hot-wire anemometers have been subjected to both analog and digital analysis, allowing extensive correlations to be made. Coherence measurements are also presented.

Nomenclature

R	= aspect ratio of nozzle
e'_1, e'_2	= fluctuating voltages from hot-wire probe
R	= correlation coefficient
t_p	= transverse dimension of nozzle
\bar{U}	= mean velocity in streamwise direction
U^*	= mean velocity in streamwise direction along centerline
V	= mean velocity in y direction
u', v', w'	= fluctuating components of velocities in x, y, z directions
x, y, z	= Cartesian coordinate as shown in Fig. 3
τ	= time lag in correlations

Subscript

0	= fixed probe position in cross correlations
---	--

Introduction

RECTANGULAR slot nozzles are used widely in such different applications as powered high lift devices for V/STOL aircraft, comfort conditioning, and effluent disposal. Frequently the jet geometry is dictated by the nature of the application. In most cases, the designer wishes to use a configuration that ensures rapid mixing of the jet flow from the nozzle. Spreading rates and mean velocity decay rates, that are gross measures of mixing rate, are also of interest.

Although plane and rectangular jet flows have been studied extensively, our understanding of the basic structure of these flows remains incomplete. A "saddle-backed" spanwise profile of mean velocity has been observed in many previous studies¹⁻⁶ of incompressible turbulent flows issuing from rectangular nozzles. Although this peculiar feature has been the subject of some discussion,³⁻⁶ it appears that the mechanism that produces these distributions is not yet understood. There is evidence that these distributions are affected strongly by the shape of the nozzle upstream of the nozzle exit plane.⁷

This work reports on continuing studies of flows from rectangular slot nozzles. The nature of the saddle-backed velocity profile problem clearly is evident in Fig. 1, which shows the total pressure field at several stations downstream in the flow from a sharp-edged rectangular orifice. Strong velocity peaks (about 20% greater than the centerline

maximum values) appear near the "ends" of the flowfield and migrate inward as one proceeds in the streamwise direction. The present study focuses attention on the peaks in the near field where they are most prominent. The work is purely experimental. Calculation procedures for three-dimensional flows are presently unable to predict the peculiar features shown in Fig. 1.^{8,9}

Much of the previous work on rectangular jets is restricted to measurements of mean velocity distributions, although some turbulence measurements are reported. In an early paper, Van der Hegge Zijnen¹ attributed saddle-backed behavior to the presence of vortices encircling the jet flow. Later, Trentacoste and Sforza³ argued that this might be only a partial explanation of those "velocity irregularities." More recently Sfieri,⁵ has taken up the encircling vortex hypothesis again, but the proposals are less than conclusive.

Several studies¹⁰⁻¹² have introduced ideas of secondary flows and vortex stretching to explain nonuniform spanwise profiles in bounded rectangular jet flows. The presence of the solid boundaries results in significant differences between the mechanisms operating in bounded flows and those in freejets, which are considered in the present work. Nonetheless, the presence of strong vorticity interactions and important secondary flow effects surely must be involved in forming saddle-backed profiles and unequal spanwise and transverse spreading rates. It is interesting to note that Viets and Sforza¹³ found that rectangular "ring" vortices showed spanwise and transverse growth patterns that are the same as those exhibited by unbounded rectangular jets: the spanwise growth rate is much less than the transverse rate, resulting in an interchange of the long axis of the field. This is sometimes referred to as crossover.

In Refs. 9 and 14, the question of pressure driven effects in rectangular jet flows is considered. The pressure field may induce secondary flows which in turn results in velocity peaks at the ends of the jet flow. The pressure field upstream of the nozzle exit plane was also cited by Owczarek and Rockwell¹¹ as the driving mechanism for secondary flows.

The present work comprises an examination of the flowfield of turbulent jets issuing from rectangular nozzles.

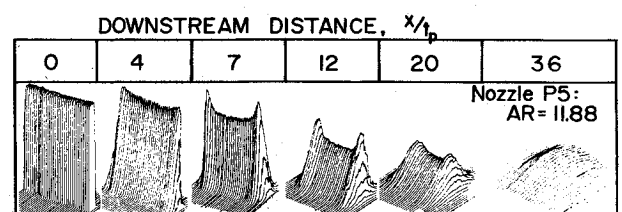


Fig. 1 Total pressure plots of flowfield at three downstream locations. Reynolds number, based on slot width t_p , approximately 40,000.

Presented as Paper 80-0202 at the AIAA 18th Aerospace Sciences Meeting, Pasadena, Calif., Jan. 14-16, 1980; submitted Jan. 16, 1980; revision received Aug. 11, 1980. Copyright © American Institute of Aeronautics and Astronautics, Inc., 1980. All rights reserved.

*Professor, Department of Mechanical Engineering. Member AIAA.

Because the saddle-backed profiles are most strongly evidenced in flows from sharp-edged orifice "nozzles," this study has concentrated on this configuration only. Moreover, all experiments were done in air at velocities low enough so that compressibility effects could be neglected. Although the static pressure field is believed to be a dominant force in producing the velocity nonuniformities, experimental work consisted of examining the resultant velocity field in the hope that this would provide some insights into the mechanisms by which saddle-backed profiles are formed.

Experimental

Experiments were carried out on jet flows issuing from rectangular orifice plate nozzles in the configuration shown in Fig. 3. Air was supplied to a settling chamber using a small commercial blower. Experiments were performed in an open laboratory area at ambient conditions. Velocities were low enough ($\approx 60 \text{ m-s}^{-1}$) so that compressibility effects were negligible. These velocities yielded jet flow Reynolds numbers, based on slot width, of the order of 50,000. The nozzle slot width was nominally 12.7 mm. Mean velocities were determined from observations of the total pressure in the

flowfield. It was assumed that the static pressure was uniform everywhere. Velocity profiles at the nozzle exit plane were very flat, with turbulence levels, $(\overline{u'^2})^{1/2}/U_{\max}$, less than about 0.6%. Centerline measurements yielded velocity decay rates that were in good agreement with the results of other experiments.^{1,3,5} The characteristic and axisymmetric decay regions^{2,3} were easily identified and are explored in more detail in Ref. 7.

Although, in the light of the distributions shown in Fig. 1, one must be careful in "centerline velocity decay" observations, the behavior of the jet centerline maximum velocity (taken at the midpoint of the spanwise and transverse profiles) with downstream distance is shown in Fig. 2 for sharp-edge orifice nozzles of four aspect ratios. Except for the lowest aspect ratio, all centerline decay plots exhibit three regimes; the potential core, characteristic decay, and axisymmetric decay, as defined in Ref. 2. Related plots of jet spreading are to be found in Ref. 7.

Mapping of the mean flowfield was done by taking observations at "grid points" across the flowfield at various downstream stations. Hot-wire anemometers were used to examine the turbulence field and to obtain correlations of the turbulence field. Two hot-wire sets were available; the outputs were not linearized, but rather used directly and reduced according to the method of Wilson.¹⁵ Standard digital and rms voltmeters were used to observe the hot-wire outputs.

The hot-wire outputs were also connected to a digital signal analyzer and a digital correlator. The signal analyzer sampled the signals at rates up to 25 KHz and digitally analyzed these data (virtually in real time) to produce amplitude spectra and coherence measurements. The correlator accepted hot-wire signals and digitally analyzed these to produce autocorrelations (for each channel) and cross-correlations for two channels of input. The lag times in both the auto- and cross-correlation analyzers could be varied over a wide range. Signal averaging, using exponential averaging, was also available.

To examine the flowfield for the presence of streamwise vortices, several techniques were tried. Wool tufts streaming in the flow were unsuccessful. The motion could not be followed, even with the aid of stroboscopic illumination. The use of crossed hot-wires was also attempted, but this procedure had to be abandoned. Even determining the local mean velocity direction in a highly sheared flow is virtually impossible. This is because, in a sheared flow, each of the wires, even though displaced only slightly, "see" different mean velocities. Yawing the probe to get equal outputs (assuming carefully matched probes) leads to incorrect results. Consider a crossed wire with the plane of the cross parallel to a wind tunnel floor, and lying in the boundary layer, along the floor centerline. The lower wire sees a lower mean velocity, and with the probe aligned with the flow, the outputs will be unbalanced. Balancing the output by yawing the probe will lead to the incorrect conclusion that the flow is skewed in the tunnel. In the flows encountered in the near fields of freejets, this complication makes finding the local mean velocity direction virtually impossible.

In the present experiments, by carefully locating the probe on the centerline of the flow, along the long axis, and within the potential core, it was possible to locate the mean velocity near the ends of the jet flow. The mean velocity direction was inclined as much as 12 deg inward (necking down) near the ends of the jet. In jets issuing from sharp-edged rectangular slots, this vena contracta effect is pronounced, and readily observable in the long-axis direction. No evidence of similar effects could be observed in the direction of the short axis. This is primarily a shortcoming of the measurement capability rather than indicating absence of such a phenomenon.

A third technique was used which incorporated one fixed and one moving wire. Wires slanted at 45 deg were used, arranged so that the wires were parallel. The fixed wire could be located at any station x_0, y_0, z_0 in the flowfield, and the

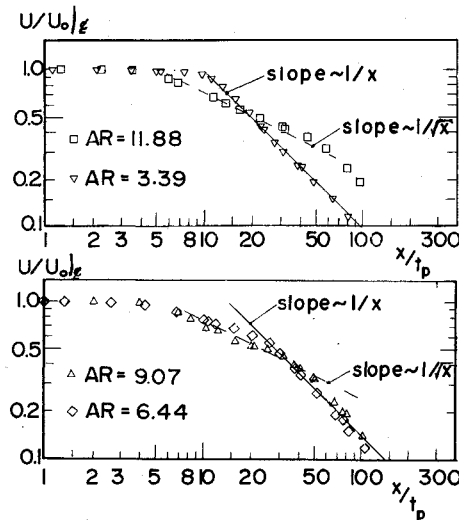


Fig. 2 Centerline velocity decay for jets issuing from sharp-edged rectangular nozzles.

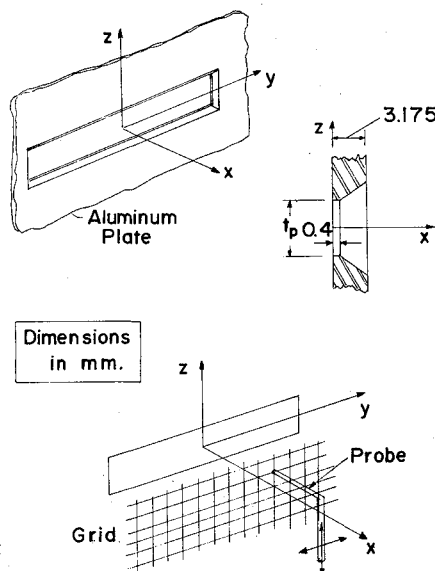


Fig. 3 Nozzle configuration and diagram of traversing grid.

moving wire could then be traversed across the flow in the z direction (parallel to the short axis). The plane of the slant wire was parallel to the x - y plane, so that these wires were sensitive to U and V components of velocity. Any strongly ordered spanwise (V component) of velocity should then appear in the form of strong correlations or anticorrelations. Both slant wires and straight wires were used in these cross-correlation traverses, so that the effect of V -component velocities could be distinguished.

Results

The peculiar feature of the saddle-backed velocity profile clearly is evident in Fig. 1. Observation of the centerline maximum velocities along the jet axis yields velocity decay plots that show the "characteristic decay" and "axisymmetric decay" regions proposed by Sforza et al.^{2,3} The merging of the peaks is not clearly evident in Fig. 1, but it has been observed⁷ that the peaks appear to merge at the same region that transition from characteristic decay gives way to axisymmetric decay. Another feature of rectangular jets, the apparent rotation of the long axis, is also not evident. This behavior is most noticeable in lower aspect ratio rectangular jets. While this rotation is expected to occur, even for aspect ratios as large as the case in Fig. 1, it occurs far downstream.

Examples of contour plots of the mean velocity distributions for these flows is shown in Fig. 4. Again, the velocity peaks are seen to be strong. The necking down of the jet is also very clear in these plots. The contour plots show fairly steady spreading in the z direction, with narrowing down, initially, in the y direction. Although contour plotting has been carried out up to about 36 slotwidths downstream no unusual features have been observed.

The velocity fields have been subjected to extensive probing using hot-wire anemometry to assist in understanding the development of these flows. The flow issues from the nozzle with very flat top hat velocity profiles (see Fig. 1) and with low levels of turbulence. The ensuing strong shear layers give rise to intense streamwise turbulence that is commonly found in jet flows. Examples of the distribution of streamwise turbulence intensity are shown in Fig. 5. Here, for two downstream stations, the turbulence intensity shows, over most of the flow, the behavior one would expect for a plane jet. At the ends of the jet, however, the end shear layer growing inward interacts with the shear layer along the "long sides" of the jet to produce peaks of intensity in the neighborhood of the velocity peaks. While this is not surprising, the nature of this distribution would probably not have been

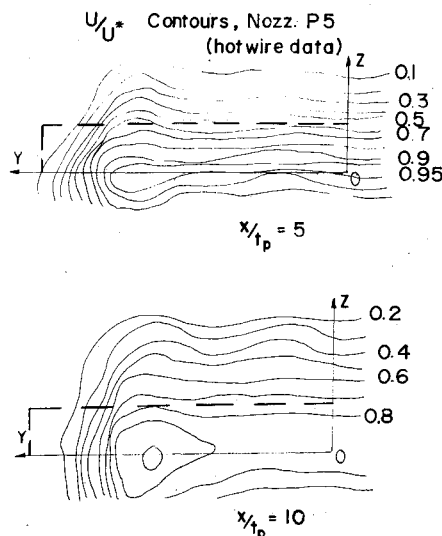


Fig. 4 Contours of streamwise mean velocity corresponding to flow shown in Fig. 1. Velocity at nozzle exit plane: 43 m/s .

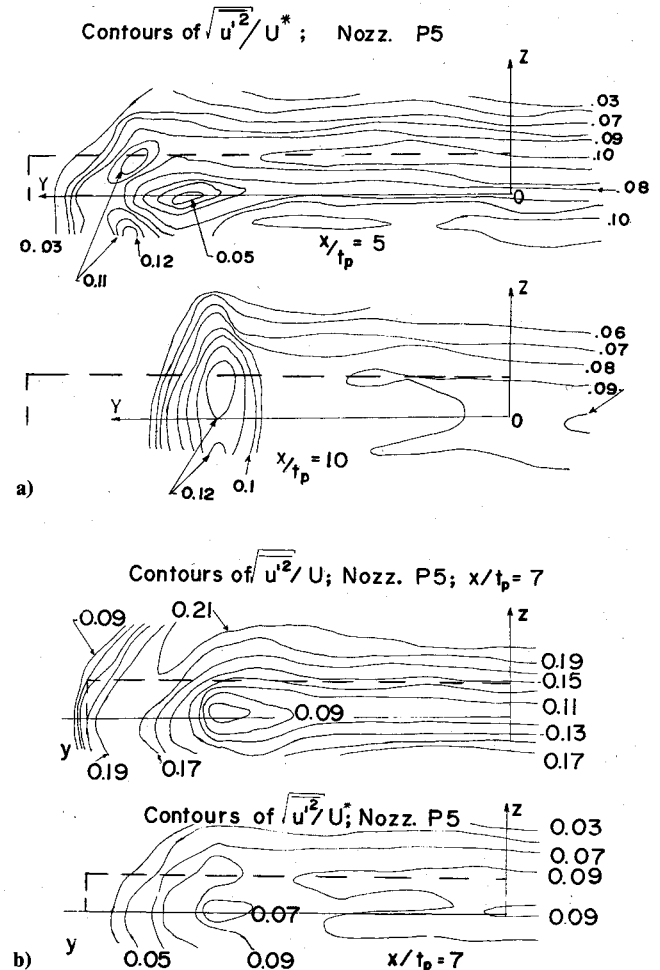


Fig. 5 Contours of streamwise turbulence intensity for flow shown in Fig. 4; a) normalized with respect to the maximum mean velocity U^* at each downstream station, b) normalized with respect to U^* and, for comparison, with the local mean velocity U .

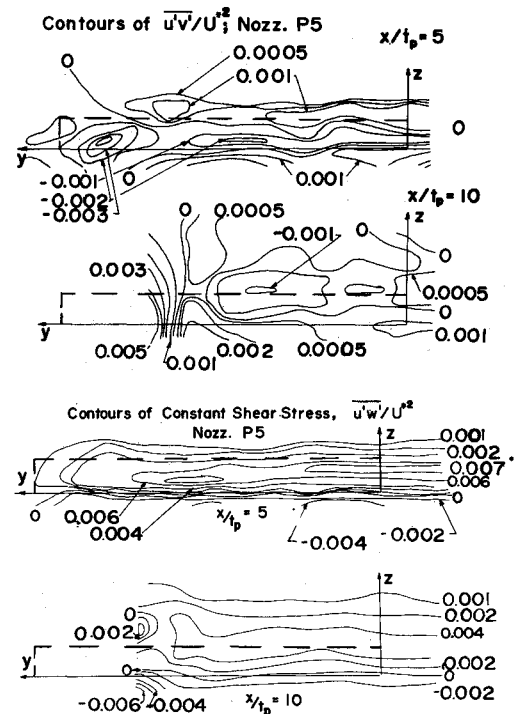


Fig. 6 Contours of the Reynolds stresses, $\overline{u'v'}/U^{*2}$ and $\overline{u'w'}/U^{*2}$ for the same conditions as Fig. 4.

predicted. However, this behavior does not explain the existence of velocity peaks, it is merely consistent with their existence.

Although crossed hot-wires were used to probe the field as well, the resulting data is of only limited value because of the difficulties in aligning the probe with the flowfield as outlined earlier. Plots of the Reynolds stresses, $\overline{u'v'}/U^*$ and $\overline{u'w'}/U^*$, are shown in Fig. 6. Care must be taken in interpreting these results. Along the long sides of the jet, the shear stresses exhibit the same general behavior as in a plane jet. At the ends however, the shear stress field becomes highly convoluted. Because the mean velocity gradients are greater here, the stresses are generally greater. Once again, there is no evidence in this structure to indicate a mechanism for velocity peaks.

By comparing the outputs of two slant wires, both oriented in the same way, it was hoped that any organized spanwise disturbances could be discerned. A fixed slant wire probe was located at three z stations successively: on the centerline, $z=0$, and at $z=0.24$ and $z=0.48$ slotwidths above the centerline. The second slant wire probe was then moved in the negative z direction while the zero delay time, R cross-correlation was recorded. Examples of the results for these cross-correlation experiments is shown in Figs. 7-9. Used in this way the correlator provided the correlations

$$R^*(\tau) = e'_1(x_0, y_0, z_0, t) \cdot e'_2(x_0, y_0, z_0 + \Delta z, t + \tau)$$

where e'_1 and e'_2 are the fluctuating voltages from the slant wires. The results, observed for $\tau=0$, were taken for various values of Δz . The minimum value of Δz was set by the proximity to which the probes could be brought safely. This

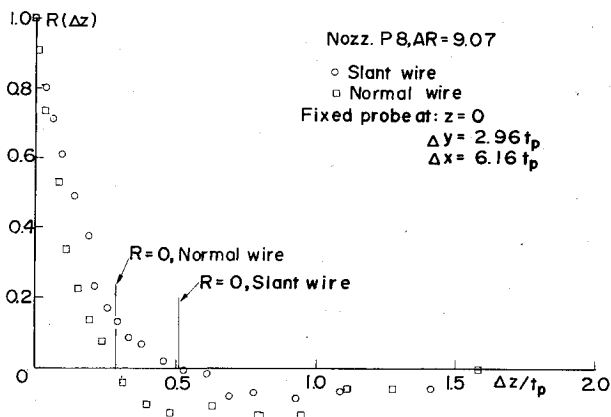


Fig. 7 Cross correlations showing results for both normal and slant wire, with fixed wire at $z=0$, and at a y station corresponding to the peak mean velocity; $Re \approx 45,000$.

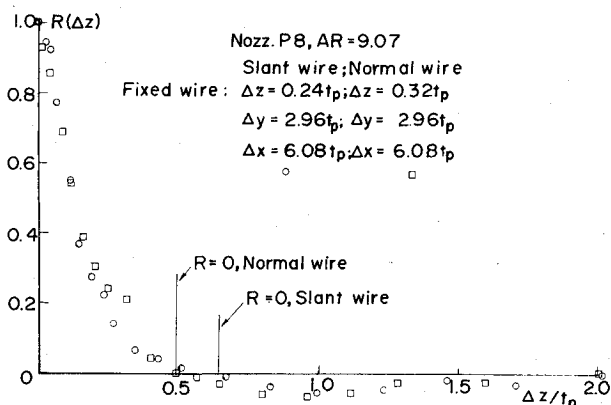


Fig. 8 Cross correlations for conditions of Fig. 7, but with fixed probe approximately one quarter slot width off the major axis.

distance was measured using a hand magnifier with an engraved scale. The raw data were plotted, and extrapolated to $\Delta z=0$ to obtain the denominator for the spatial cross-correlation coefficient $R(\Delta z)$

$$R(\Delta z) = R^*(0) / e'_1(x_0, y_0, z_0, 0) \cdot e'_2(x_0, y_0, z_0 + \Delta z, 0)$$

Although some error is inherent in this procedure, all of the data are affected in the same way; the error is considered to be small in any event.

In Fig. 7 we compare the correlations for the slant wire and the straight wire at a y displacement corresponding very nearly to the velocity peak location (i.e., $y/t_p = 2.96$). The fixed probe is at the jet centerline, while the moving probe moves in the direction $-z$. Positive correlation persists over a considerably greater distance in the slant probe case. In Fig. 8, the slant and straight wire probes are compared for the same y station but with z_0 located roughly one quarter slot width above the centerline of the flow. In Fig. 9, the fixed probe is approximately one half the slot width above the centerline, while the y location is held constant. In all cases, the value of Δz at which $R=0$ (for several values of y) is larger for the slant wire, indicating that there is some mechanism by which correlation of lateral flows persists longer than for the case of longitudinal fluctuations only. The average value of the ratio of $\Delta z_{R=0}$ for the slant wire to $\Delta z_{R=0}$ for the straight wire was 1.36. If strong streamwise vortices exist, one would have expected fairly strong positive correlations for the case shown in Fig. 9, at values of Δz near unity. The data, which are subject to some error, especially at large Δz , do not show strong trends toward such positive correlations.

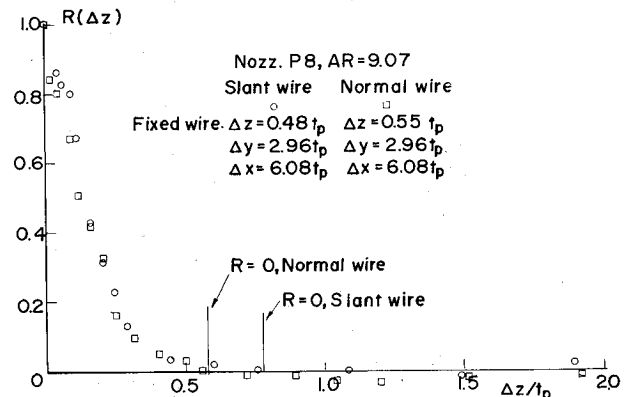


Fig. 9 Cross correlations for conditions of Fig. 7, but with fixed probe approximately one half slot width off the major axis.

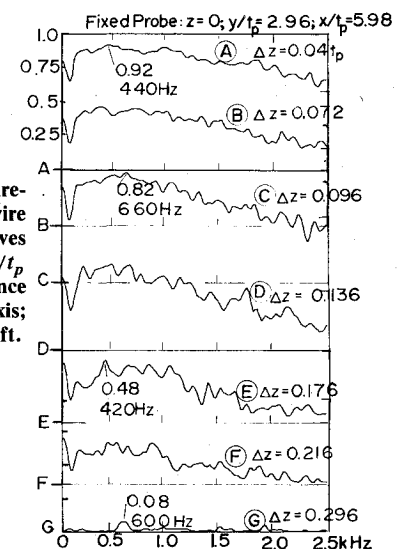


Fig. 10 Coherence measurements with fixed slant wire probes on major axis. Curves for different values of $\Delta z/t_p$ are labeled to identify reference baseline on left-hand axis; interval scale shown at top left.

The evidence of persistence of correlation over greater z -wise distances is further examined in the coherence data shown in Fig. 10. Sample plots of the coherence as a function of frequency are shown. The coherence function is a measure of cause-effect relationships,¹⁶ and would be expected to give values near unity if the velocity fluctuations measured at two points in the flow are caused by the same mechanism. The data in Fig. 10 were taken with the fixed slant wire probe at $z=0$, $y/t_p=2.96$ and $x/t_p=5.98$. The coherence falls off rapidly with increased probe separation, falling to virtually zero when the moving probe is 0.3 slot widths below the centerline. With the fixed probe near the upper edge of the jet, however, ($z/t_p=0.502$), the coherence function first shows a more rapid decrease with both frequency and distance, but the levels of coherence are still appreciable at separations of almost one slot width. Although these effects are weak, the trends suggest that the velocity fluctuations at $\Delta z=1.0 t_p$ may be related.

Discussion

In a series of experiments on rectangular jet flows, turbulence measurements indicate straight-forward behavior in the shear layers on the long sides of the jets. Near the ends of the jets, however, the intensity of turbulence is much increased as the two shear layers growing on the jet ends and sides interact.

The velocity peaks which appear near the ends of the jets cannot be explained in terms of the turbulence stresses alone. There is no mechanism in the normal and shearing stresses to account for these peaks.

In view of the fairly high curvature of streamlines between the nozzle exit plane and the vena contracta it seems clear that significant variations of static pressure must occur. One must then question the assumption of constant static pressure, which is inherent in viewing the distributions in Fig. 1 as being representative ($U \propto \sqrt{\Delta p}$) of mean velocity distributions. However, hot-wire data show the same peaks. The pressure field associated with curved streamlines would have a peak value along the centerline ($x-z$) in the jet flow. This centrally located high pressure region could drive secondary flows that could move high velocity fluid from the central one to the outer ends of the flowfield. Until satisfactory means become available for precise determination of static pressures in turbulent free shear flows, this suggestion is purely speculative. Nonetheless, the likelihood of secondary flows as a dominant mechanism looms large.

The flowfield was examined at a single downstream station using 45 deg slant hot-wire probes and examining the spatial cross correlation of the fluctuating signal from the probes. Such an arrangement should be sensitive to cross-stream velocities. Except for some small but reproducible differences in the spatial separation at which the cross correlation drops to zero (a measure of the scale of the turbulent fluctuations), and some minor effects noticed in coherence measurements, little evidence has been acquired to show the existence of strong streamwise vortices.

Conclusions

Experiments conducted on rectangular jets show intense turbulence activity at the ends of the jet. Despite extensive probing of the flowfield, the mechanism which produces saddle-backed velocity profiles has not been determined.

Acknowledgments

This work has been supported by the National Research Council of Canada, under Grant A4310. Additional financial support provided by the School of Graduate Studies and Research of Queen's University is gratefully acknowledged.

References

- ¹Van der Hegge Zijnen, B. G., "Measurements of the Velocity Distribution in a Plane Turbulent Jet of Air," *Applied Science Research, Section A*, Vol. 7, 1958, pp. 256-276.
- ²Sforza, P. M., Steiger, M. H., and Trentacoste, N., "Studies on Three-Dimensional Viscous Jets," *AIAA Journal*, Vol. 4, May 1966, pp. 800-806.
- ³Trentacoste, N. and Sforza, P., "Further Experimental Results for Three-Dimensional Free Jets," *AIAA Journal*, Vol. 5, May 1967, pp. 885-891.
- ⁴Sfieri, A. A., "The Velocity and Temperature Fields of Rectangular Jets," *International Journal of Heat and Mass Transfer*, Vol. 19, 1976, pp. 1289-1297.
- ⁵Sfieri, A. A., "Investigation of Three-Dimensional Turbulent Rectangular Jets," *AIAA Journal*, Vol. 17, Oct. 1979, pp. 1055-1060.
- ⁶Krothapalli, A., Baganoff, D., and Karamcheti, K., "Turbulence Measurements in a Rectangular Jet," AIAA Paper 79-0074, New Orleans, La., Jan. 1979.
- ⁷Marsters, G. F., "The Effects of Upstream Nozzle Shaping on Incompressible Turbulent Flows from Rectangular Nozzles," *Transactions of CSME*, Vol. 4, 1978/79, pp. 197-203.
- ⁸Oh, Y. H. and Harris, J. E., "Numerical Solutions of Three-Dimensional Free Turbulent Shear Flows," *Symposium on Turbulent Shear Flows*, University Park, Penn., Vol. 1, April 1977, pp. 1.17-1.28.
- ⁹McGuirk, J. J. and Rodi, W., "The Calculation of Three-Dimensional Turbulent Free Jets," *Symposium on Turbulent Shear Flows*, University Park, Penn., Vol. 1, April 1977, pp. 1.29-1.36.
- ¹⁰Foss, J. F. and Jones, J. B., "Secondary Flow Effects in a Bounded Rectangular Jet," *Journal of Basic Engineering, Transactions of the ASME*, June 1968, pp. 241-249.
- ¹¹Owczarek, J. A. and Rockwell, K. O., "An Experimental Study of Flows in Planar Nozzles," *Journal of Basic Engineering, Transactions of the ASME*, Sept. 1972, pp. 682-688.
- ¹²Rockwell, D. O., "Vortex Stretching Due to Shear Layer Instability," *Journal of Fluids Engineering, Transactions of the ASME*, March 1977, pp. 240-244.
- ¹³Viets, H. and Sforza, P. M., "Dynamics of Bi-laterally Symmetric Vortex Rings," *Physics of Fluids*, Vol. 15, Feb. 1972, pp. 230-240.
- ¹⁴Tjonneland, J. and Birtch, S. F., "Applications of Viscous Analyses to the Design of Jet Exhaust Powered Lift Installations," 1979 Israel Gas Turbine Congress, Haifa, Israel, July 1979.
- ¹⁵Wilson, D. J., "An Experimental Investigation of the Mean Velocity, Temperature and Turbulence Fields in Plane and Curved Two-Dimensional Wall Jets Coanda Effect," Ph.D. Thesis, Univ. of Minnesota, 1970.
- ¹⁶Strahle, W. C., "Generalized Time Series Analysis in Turbulent Combustion Research," AIAA Paper 79-0020, New Orleans, La., Jan. 1979.